Contribution of the 30/36 Hydrophobic Contact at the C-Terminus of the α-Helix to the Stability of the Ubiquitin Molecule†

Susan T. Thomas and George I. Makhatadze*

Department of Biochemistry and Molecular Biology, Pennsylvania State University College of Medicine, Hershey, Pennsylvania 17033

Received January 10, 2000; Revised Manuscript Received June 6, 2000

ABSTRACT: The contribution of the hydrophobic contact in the C-capping motif of the α-helix to the thermodynamic stability of the ubiquitin molecule has been analyzed. For this, 16 variants of ubiquitin containing the full combinatorial set of four nonpolar residues Val, Ile, Leu, and Phe at C4 (Ile30) and C″ (Ile36) positions were generated. The secondary structure content as estimated using far-UV circular dichroism (CD) spectroscopy of all but Phe variants at position 30 did not show notable changes upon substitutions. The thermodynamic stability of these ubiquitin variants was measured using differential scanning calorimetry, and it was shown that all variants have lower stability as measured by decreases in the Gibbs energy. Since in some cases the decrease in stability was so dramatic that it rendered an unfolded protein, it was therefore concluded that, despite apparent preservation of the secondary structure, the 30/36 hydrophobic contact is essential for the stability of the ubiquitin molecule. The decrease in the Gibbs energy in many cases was found to be accompanied by a large (up to 25%) decrease in the enthalpy of unfolding, particularly significant in the variants containing Ile to Leu substitutions. This decrease in enthalpy of unfolding is proposed to be primarily the result of the perturbed packing interactions in the native state of the Ile → Leu variants. The analysis of these data and comparison with effects of similar amino acid substitutions on the stability of other model systems suggest that Ile → Leu substitutions cannot be isoenergetic at the buried site.

Analysis of known protein structures have revealed the existence of specific preferences of amino acid residues to certain secondary structure elements and specific topological arrangements of secondary structure (*1*, *2*). The so-called helix-capping interactions at the end of α-helices are probably one of the best characterized (*3*). The hydrogen bonding between amide hydrogen bond donors and carbonyl oxygen acceptors of residues situated four apart in the sequence is the main structural element of the α-helix (*4*). This pattern of hydrogen bonding, however, implies that four initial amide hydrogen bond donors and the last four carbonyl oxygen hydrogen bond acceptors do not have hydrogen-bonding partners. Stereochemical (*5*) and statistical (*6*) analyses of the amino acid residues at the ends of α-helices revealed the existence of the specific capping interactions at both the N- and C-termini, which compensate for the unsatisfied hydrogen bonds and thus prevent the ends from fraying. These capping box motifs provide favorable interactions facilitating helix initiation and termination and include hydrogen-bonding (both backbone−backbone and side chain−backbone) and hydrophobic interactions.

Observations of specific interactions at the ends of α-helices stimulated experimental work in this field [see Aurora and Rose (*3*) for references]. However, only a few addressed the question of the hydrophobic interaction in the helix termination (*7*−*9*). The model host peptide studied by Kallenbach's group (*7*) had the sequence Ac-YMSEDEL-KAAEAAFKHNGVP-NH_2. Structural analysis using ^{1}H NOESY experiments showed that this peptide forms a classical α_L C-capping motif (*3*) with a backbone−backbone hydrogen bond between Gly18 and Lys15 and a hydrophobic contact between the side chains of Phe14 and Pro20. In the other model peptide study, Sukumar and Gierasch (*8*) used a helical peptide derived from the cellular retinoic acid binding protein. They were able to show that the hydrophobic interactions at the C-terminus occur even in the isolated peptide and that the presence of these interactions induces efficient helix termination. In contrast, Viguera and Serrano (*9*) concluded that the C-capping motif is not populated to a large extent in aqueous solution. They used a host peptide, YGGSKAEAARAX1AKHGX2GG-NH_2, with the positions X1 and X2, which were supposed to form a hydrophobic contact, replaced by the nonpolar residues Gly, Ala, Val, Ile, Leu, Met, and Phe. This conclusion, however, does not undermine the possibility that when a helix is incorporated into a protein structure, interactions with the rest of the protein will provide additional stabilization. All of these experimental studies do not provide convincing evidence for the importance of the hydrophobic interaction for helix termination at the C-terminus. However, no systematic experimental thermodynamic study of such interactions, particularly in a protein system, has been performed. A

† This work was supported by Research Grant GM54537 (G.I.M.) from the National Institutes of Health and by the Petroleum Research Fund, Grant 31279-G4 (G.I.M.), administered by the American Chemical Society.

* To whom correspondence should be addressed. E-mail: makhatadze@psu.edu. Phone: (717) 531-0712. Fax: (717) 531-7072.

10.1021/bi0000418 CCC: $19.00
Published on Web 07/27/2000

complete quantitative understanding of the stereochemical basis of helix capping will depend on the availability of precise thermodynamic information on different amino acid residues in hydrophobic positions of capping boxes of α-helices. The mutational studies of helix-capping interactions within protein structures can provide this information. Because protein unfolding is a two-state process, thermodynamic analysis of the effect of the substitutions on the stability of a single domain protein is straightforward. We chose the α-helix of ubiquitin as a model system for such studies.

The ubiquitin molecule is a suitable protein model system. This is a small (76 amino acid residues) globular protein which does not contain any disulfide bonds and does not bind cofactors, is readily soluble in aqueous solution, and unfolds reversibly in a two-state manner under both equilibrium and kinetic conditions (*10*, *11*). The secondary structure of ubiquitin consists of five *β*-strands forming a somewhat concave surface (*12*). An α-helix that includes residues 23−34 lies on the sheet part of the molecule (*13*). This α-helix of three full turns has both N-capping and C-capping interactions. The α_L capping motif at the C-terminus of the α-helix of ubiquitin has the backbone−backbone hydrogen bond between residues Gly35 (C′) and Gln31 (C3) and hydrophobic interactions between residues Ile30 (C4) and Ile36 (C″). The side chains of Ile30 and Ile36 are in close van der Waals contact in the native state of the ubiquitin molecule.

In this paper we report the results of thermodynamic analysis of the stability of the ubiquitin variants containing amino acid substitutions at positions 30 (Ile30) and 36 (Ile36). Sixteen variants of ubiquitin containing the full combinatorial set of Val, Ile, Leu, and Phe at these two positions were generated, their stability was measured using differential scanning calorimetry (DSC),[1] and their secondary structure content was estimated using far-UV circular dichroism (CD) spectroscopy. We show that 30/36 hydrophobic contact is important for the stability of the ubiquitin molecule. This hydrophobic contact does not, however, seem to have significant effect on the secondary structure content as measured by CD spectroscopy.

MATERIALS AND METHODS

Mutagenesis and Expression of Ubiquitin Variants. Site-directed mutagenesis of the yeast ubiquitin gene was carried out as described by Cormack (*14*) or by using the QuickChange Site-Directed Mutagenesis kit (Stratagene). The presence of mutations was confirmed by sequencing the entire ubiquitin gene using an Applied Biosystems PRISM 310 genetic analyzer. Overexpression of the ubiquitin variants was done in the BL21(DE3) strain of *Escherichia coli* as described elsewhere (*15*). Each variant was purified to apparent homogeneity using ammonium sulfate precipitation followed by ion-exchange and gel filtration chromatographies as previously described (*11*). For the reason described previously (*11*), all described ubiquitin variants contained Arg63Lys substitution.

Circular Dichroism (*CD*) *Spectroscopy*. CD spectra of the ubiquitin variants at 25 °C were measured on a Jasco J-715 spectropolarimeter as described elsewhere (*15*, *16*). Each spectrum was accumulated at least twice and resulted from averaging five successive individual spectra. Water-jacketed 1 mm cylindrical quartz cells were used in all experiments. Solutions of the ubiquitin variants in CD buffer (10 mM NaCl, 1 mM sodium phosphate, 1 mM sodium citrate, 1 mM sodium borate, pH 3.0) had protein concentrations of 0.05−0.2 mg/mL. Measured values of the ellipticity, Θ, were normalized by protein concentration, *c*, and converted into molar ellipticity per amino acid residue base, [Θ], as

$$[\Theta] = \frac{\Theta M_{aar}}{lc} \tag{1}$$

where *i* is the optical length of the cell and M_{aar} is the average mass of the amino acid residues in ubiquitin taken as 110 Da.

Differential Scanning Calorimetry (*DSC*). DSC experiments were performed on a VP-DSC (Microcal Inc., Northhampton, MA) instrument at a scan rate of 1 deg/min. The protein concentration for ubiquitin mutants varied between 1 and 5.0 mg/mL depending on the experimental pH. The buffer systems used were 10 mM glycine hydrochloride in the pH range from 2.0 to 3.25 and 10 mM sodium acetate in the pH range from 3.5 to 4.5. Detailed procedures of the sample preparation for the DSC experiment were the same as described in ref *17*. In specially designed experiments, it was shown that the reversibility of unfolding in most cases was better than 90% and that there was no notable dependence of the DSC profiles on the protein concentration. The partial molar heat capacity of the protein, $C_{p,pr}(T)$, was obtained from the experimentally measured apparent heat capacity difference between the sample (containing protein solution) and reference (containing corresponding buffer solution) cells, $\Delta C_p^{app}(T)$, using the expression:

$$C_{p,pr}(T) = \frac{C_{p,buf}}{\bar{V}_{buf}}\bar{V}_{pr} - \frac{\Delta C_p^{app}(T)}{m_{pr}M} \tag{2}$$

where $\bar{V}_{pr}$ is the partial molar volume of a protein calculated as described (*18*), $C_{p,buf}$ and $\bar{V}_{buf}$ are the partial molar heat capacity and the partial molar volume of the aqueous buffer, respectively, m_{pr} is the mass of the protein in the cell, and *M* is the molar mass of the protein.

Protein concentration was measured spectrophotometrically using a known extinction coefficient for the wild-type ubiquitin, $\epsilon^{0.1\%}_{1cm,276nm} = 0.149$ (*11*). This extinction coefficient was used for all ubiquitin variants since none of the amino acid substitutions introduced tyrosine or tryptophan which strongly absorbs in the far-UV range. Correction for light scattering was taken into account as described (*19*). Analysis of the heat capacity profiles was done using the nonlinear regression routine NLREG and in-house written scripts (*17*). All curves for a given ubiquitin variant were fit simultaneously to a two-state transition model using common functions for the heat capacities of the native and the unfolded states and with enthalpy of unfolding, ΔH^{exp}, heat capacity of unfolding, ΔC_p, and transition temperature, T_m, as independent variables (*17*). In cases where the contribution of the cold denaturation was particularly significant, we used the temperature where the entropy function crosses zero as the reference temperature (*20*). The standard thermodynamic

[1] Abbreviations: CD, circular dichroism; DSC, differential scanning calorimetry; ASA, water-accessible surface area.

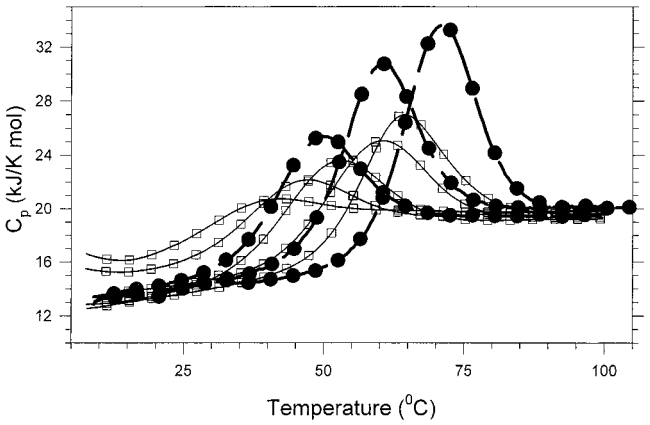

FIGURE 1: Partial molar heat capacity profiles for the wild-type ubiquitin (dashed lines and filled circles) and 30V/36L variant (solid lines and open squares). Each profile was obtained at a different solution pH: from left to right for WT, pH = 2.5, 3.0, and 3.5, and for 30V/36L, pH = 2.75, 3.0, 3.25, 3.5, and 3.75. Symbols show the results of the simultaneous fit of the data to a two-state transition as described in Materials and Methods, using the parameters listed in Table 1.

functions under reference conditions were calculated as

$$\Delta H^{\exp}(T) = \Delta H(T_m) + \Delta C_p(T - T_m) \quad (3)$$

$$\Delta S(T) = \Delta S(T_m) + \Delta C_p[\mathrm{d}\ln(T/T_m)] = \frac{\Delta H^{\exp}(T_m)}{T_m} + \Delta C_p[\mathrm{d}\ln(T/T_m)] \quad (4)$$

$$\Delta G(T) = \Delta H^{\exp}(T_m) - T\frac{\Delta H(T_m)}{T_m} + \Delta C_p(T - T_m) - T\Delta C_p[\ln(T/T_m)] \quad (5)$$

where $\Delta S(T)$ and $\Delta G(T)$ are the entropy and Gibbs energy functions of a protein, respectively.

RESULTS AND DISCUSSION

Figure 1 shows the partial molar heat capacity profiles for the WT and one of the variants (30V/36L) of ubiquitin in solutions with different pH values. Several notable features can be observed. First, at the same pH value of the solution, the 30V/36L variant unfolds at a lower temperature than the wild-type protein. For example, at pH 3.5 the transition temperature of WT is ~71 °C. For the 30V/36L variant the transition temperature is more than 15 deg lower. Second, the enthalpy of unfolding, which is represented by the area under the heat capacity profile, is significantly lower for the 30V/36L variant. Indeed, we can compare two profiles, WT at pH 3.0 and 30V/36L at pH 3.5, for which the unfolding temperatures are very similar. When compared at the same temperatures, the area under the heat capacity profile is much smaller for the 30V/36L variant, providing direct indication that the enthalpy of unfolding of WT is significantly higher than for the 30V/36L variant. Third, the 30V/36L variant clearly undergoes cold denaturation under the conditions where the WT protein does not. The apparent partial molar heat capacity of the 30V/36L variant at 25 °C increases with the decrease in pH. At pH 2.75 the heat capacity profile actually curves upward at low temperatures, clearly indicating the contribution from the cold denaturation. Cold denaturation in human ubiquitin was observed by us previously (*20*). However, in the case of human ubiquitin, cold denaturation was observed upon addition of a chemical denaturant which, in addition to lowering the transition temperature, is known to decrease the enthalpy of unfolding as well (*21*). Direct observation of the cold denaturation for the 30V/36L variant confirms that the observed decrease in the transition temperature and decrease in the enthalpy of unfolding are not fictitious but are induced by the amino acid substitutions at 30/36 positions. Fourth, the partial molar heat capacities for both WT and the 30V/36L variant in the native and unfolded states are clustered close despite the differences in the transition temperatures and the enthalpies of unfolding. The close correspondence between the heat capacities for WT and the 30V/36L variant indicates that at least in a first approximation the heat capacity changes upon unfolding, ΔC_p, of these two proteins are comparable (*22*).

Detailed results of the thermodynamic analysis of the ubiquitin variants with all the possible combinations of Ile, Val, Leu, or Phe at positions 30 and 36 are presented in Table 1. The data for each variant have been obtained in most cases under several solvent conditions. This is very important because it allows a direct estimate of the heat capacity change upon unfolding, ΔC_p, for each variant using the dependence of the enthalpy of unfolding, $\Delta H^{\exp}$, on transition temperature, T_m. The values of ΔC_p are important for the calculations of the enthalpy, entropy, and Gibbs energy functions of a protein at any temperature using the standard thermodynamic relationships in eqs 3−5 (e.g., ref *22*). No experimental DSC data are reported for 30F/36F and 30F/36L variants of ubiquitin. In addition to their intrinsically low solubility in aqueous solution, DSC experiments did not produce a heat absorption peak, indicating extremely low stability of the 30F/36F and the 30F/36L variants under the solvent conditions studied (pH 2.0−4.5).

To facilitate comparison of different ubiquitin variants, we had to choose common "standard conditions". The standard conditions were defined as pH 3.0 and 50 °C because they represent the median values for all of the DSC data collected on the ubiquitin variants. Table 2 presents the comparison of the transition temperature, T_m at pH 3.0, the enthalpy of unfolding, $\Delta H^{\exp}$ at 50 °C, and the heat capacity change upon unfolding, ΔC_p. There are two major trends typical for all variants.

Effect of 30/36 Amino Acid Substitutions on the Enthalpy of Unfolding. The first trend is that in several cases the amino acid substitutions led to a statistically significant (>15%) decrease in the enthalpy of unfolding (Table 2). In particular, almost all (five out of six, with the exception of the 30L/36F variant) variants containing the Leu residue have considerably lower enthalpy by as much as 40 kJ/mol or almost 25% of 170 kJ/mol of the unfolding enthalpy for the WT (30I/36I) protein. This decrease in enthalpy is not exclusive for the variants containing Leu residues. For example, 30V/36V also has a lower enthalpy of unfolding. Similar decreases in the enthalpy of unfolding upon amino acid substitutions, although much smaller, 5−9%, have been observed before for several proteins (*23*−*30*). Currently, there is not much computational potential for predicting the changes in the enthalpy of unfolding even using the detailed 3D structure of proteins. This is even less feasible in our case since we do not yet have detailed information on the

Table 1: Thermodynamic Parameters of Unfolding of 30/36 Variants of Ubiquitin Measured Using Differential Scanning Calorimetry[a]

pH	T_m[b] (°C)	$\Delta H^{exp}(T_m)$ (kJ/mol)	$\Delta H^{fit}(T_m)$ (kJ/mol)	pH	T_m (°C)	$\Delta H^{exp}(T_m)$ (kJ/mol)	$\Delta H^{fit}(T_m)$ (kJ/mol)
	30I/36I (WT)					30V/36L	
2.00	39.8	144	140	2.50	11.5		0
2.50	46.9	157	162	2.75	24.2	41	42
2.50	46.5	157	145	3.00	35.9	88	85
2.75	52.5	187	171	3.25	48.0	128	140
3.00	59.3	203	198	3.50	56.0	175	159
3.25	68.3	230	235	3.75	56.4	154	160
3.50	70.1	248	243	4.00	61.9	160	179
3.50	71.2	243	249				
	30L/36L					30V/36V	
2.50	12.7		0	2.50	11.2		0
2.75	33.5	80	81	2.75	35.6	87	94
3.00	46.2	130	125	3.00	46.7	137	136
3.25	54.2	157	146	3.25	53.5	148	151
3.50	62.7	170	168	3.50	62.5	172	174
	30L/36I					30V/36I	
2.50	11.7		1	2.50	32.9	90	94
2.75	35.2	84	88	2.75	41.2	127	133
3.00	46.8	122	127	3.00	49.4	139	160
3.25	54.5	134	147	3.25	54.8	170	166
3.50	55.4	165	161	3.50	61.6	203	205
4.50	62.7	184	186				
	30L36V					30V/36F	
2.25	10.7		0	2.50	24.5	56	62
2.50	31.0	83	79	2.75	31.7	96	96
2.75	41.1	96	115	3.00	39.6	106	124
3.00	50.6	138	147	3.25	48.3	159	158
3.25	58.7	169	171	3.50	55.7	178	180
	30L/36F					30F/36V	
2.25	32.6	84	93	3.00	30.2	76	68
2.50	36.9	103	109	3.25	40.3	111	119
2.75	44.4	136	142				
3.00	53.3	165	171				
3.25	59.8	188	186				
	30I/36L					30F/36I	
2.5	36.6	98	106	3.00	23.3	46	59
2.75	39.3	107	103	3.50	32.4	79	75
3	50.6	146	150	4.00	54.4	130	120
3.25	58.2	164	161	4.00	53.4	134	135
3.5	64.1	177	183				
	30I/36V					30I/36F	
2.25	32.5	95	100	2.50	43.5	133	146
2.50	40.4	123	125	2.75	48.7	148	161
3.00	56.1	184	183	3.00	55.5	175	186
3.25	64.3	200	202	3.25	60.4	213	200
3.50	69.5	208	215	3.50	66.1	212	216

[a] The estimated errors for the reported thermodynamic parameters are as follows: for the transition temperature, T_m, the error of measurements is less than 1 deg, the calorimetric enthalpy of unfolding, ΔH^{exp}, has an uncertainty of less than 5−7% and is largely due to the uncertainties of concentration measurements, and the fitted enthalpy for a two-state transition, $\Delta H^{fit}(T_m)$, has an error bar of less than 5 kJ/mol. [b] The underlined values represent not the transition temperature but the remperature at which the entropy change is zero (see Materials and Methods for details). In this case the calorimetric enthalpy cannot be obtained experimentally.

Table 2: Comparison of the Standard (50 °C, pH 3.0) Thermodynamic Parameters of 30/36 Variants of Ubiquitin

variant ID	T_m[a] (°C)	ΔC_p[b] [kJ/(mol·K)]	ΔH^{exp} (50 °C)[c,d] (kJ/mol)	ΔG(50 °C, pH 3.0) (kJ/mol)	$[\Theta]_{222}$ (deg·cm^2·dmol^{-1})	R_2
30I/36I (WT)	59.8	3.4	170 (0%)	5.9	−4250	−2.3
30I/36F	54.8	3.9	157 (8%)	2.3	−4380	−1.9
30I/36L	49.8	2.9	138 (19%)	0.4	−4400	−2.1
30I/36V	55.6	3.2	156 (8%)	2.6	−4880	−2.1
30L/36F	52.5	3.8	153 (10%)	0.5	−4950	−1.9
30L/36I	45.5	3.6	135 (21%)	−2.3	−4310	−2.1
30L/36L	44.4	3.2	139 (18%)	−2.2	−4190	−2.2
30L/36V	50.0	3.2	136 (20%)	0.0	−3950	−2.1
30V/36F	40.0	3.9	158 (7%)	−4.5	−4250	−2.2
30V/36I	48.0	3.8	156 (8%)	−0.7	−4490	−2.1
30V/36L	36.0	3.5	137 (19%)	−5.1	−4350	−2.0
30V/36V	45.2	3.1	138 (19%)	−1.9	−4120	−2.1
30F/36V	30.2	3.5	146 (14%)	−7.4	−4490	−2.7
30F/36I	21.6	2.9	120 (29%)	−8.0	−3900	−2.2
30F/36L	ND[e]	ND	ND	−11.5 to −10.0	−390	−6.4
30F/36F	ND	ND	ND	−14.2 to −12.7	−1700	−2.7

[a] The transition temperature at pH = 3.0 was calculated from the linear fit of the experimental T_m versus pH data shown in Table 1. [b] The heat capacity change was calculated as a slope of the linear fit of the experimental ΔH^{exp} versus T_m data shown in Table 1. [c] The enthalpy of unfolding at the transition temperature shown in the second column was calculated from the linear fit of the experimental ΔH^{exp} versus T_m data shown in Table 1. [d] Values in parentheses indicate the difference of the calorimetric enthalpy of a given variant from that of the WT protein. [e] ND, not deteremined.

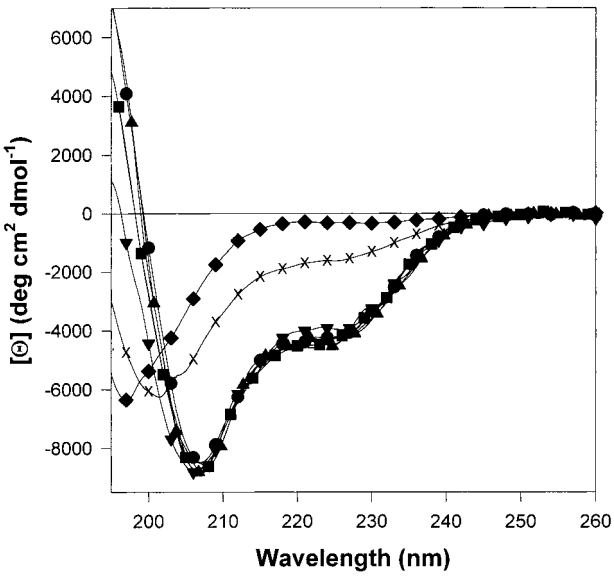

FIGURE 2: Far-UV CD spectra of the ubiquitin variants at 25 °C and pH 3.0: WT (●), 30V/36L (■), 30F/36I (▼), 30I/36L (▲), 30F/36L (◆), and 30F/36F (×).

structures of our 30/36 ubiquitin variants. It is clear, however, that the changes in the structures are not very dramatic. This conclusion follows from the comparison of the far-UV CD spectra of these ubiquitin variants (Figure 2). Circular dichroism spectroscopy is a useful tool in monitoring global changes in protein secondary structure at a low resolution (*31*). It has been used successfully for deriving helix propensity parameters in isolated helical peptides in solution (e.g., refs *32*−*40*). In an attempt to see whether there are significant changes in the secondary structure of the ubiquitin molecule, far-UV CD spectra of WT and variants of ubiquitin were recorded.

Figure 2 compares the far-UV CD spectrum for WT ubiquitin with the spectra of selected variants, 30V/36L, 30I/36L, and 30F/36I. These three variants were selected because they have very distinct transition temperatures and unfolding enthalpies from those of WT. Despite the difference in the thermodynamic properties, the spectra of ubiquitin variants are very similar, indicating that probably there is little, if any, change in the secondary structure of these proteins. Table 2 compares the mean residue ellipticity at 222 nm for

all 30/36 variants. There is some variation in the absolute values from −3950 to −4950 deg·cm^2·dmol^{-1}. However, the standard deviation around the average value of −4500 deg·cm^2·dmol^{-1} is on the order of 8%, comparable to usual 5−10% estimates of the error in the ellipticity measurements (*41*). Comparison of small changes in the ellipticity is sometimes problematic, however, because the absolute values depend on the accuracy of the concentration measurements. This is in particular a significant obstacle in our case, keeping in mind the low extinction coefficient for ubiquitin and the low concentrations (0.2−0.05 mg/mL) used in our CD experiments. To avoid this problem, a parameter, which reflects the ratio of intensities at two wavelengths, has been introduced (*42*). From the CD spectra presented in Figure 2, we derived the parameter, R_2, as the ratio of minimum intensity in the range from 195 to 210 nm to the intensity at 222 nm (Table 2). Interestingly, as judged by similarities in R_2, the amino acid substitutions at the 30/36 positions did not lead to changes in the secondary structure of the ubiquitin molecule (with the exceptions of 30F/36F, 30F/36L, and 30F/36V, which are somewhat prone to aggregation). It should be mentioned, however, that the R_2 parameter has been shown to be a useful measure for the amount of helical structure in isolated peptides (*9*) but has never been applied to protein helices.

If the secondary structure of the 30/36 variant of ubiquitin remains unchanged, what then is causing the decrease in the enthalpy of unfolding? It is believed from both experimental and theoretical considerations (*43*, *44*) that the enthalpy of protein unfolding in an aqueous solution, ΔH^{exp}, can be divided into two parts. One part is associated with the interactions in the protein interior, $\Delta_N^U H^{int}$, and the other part is associated with the enthalpy of interactions of internal protein groups with water upon exposure due to unfolding, $\Delta_N^U H^{hyd}$. The enthalpies of internal interactions originate from hydrogen bonding and van der Waals interactions. The latter is sometimes also referred to as packing interactions (*45*, *46*). These packing interactions are of particular importance in the case of the 30/36 ubiquitin variants because they are nonpolar by design and presumably they do not affect the hydrogen-bonding network. It is important to mention that the internal interactions contribute positively to the enthalpy of unfolding, whereas the enthalpy of hydration has a negative contribution (*43*, *44*). Thus the enthalpy of internal interactions and the hydration enthalpy will be compensating each other.

The hydration term can be approximated as being proportional to the change in the water-accessible surface area upon protein unfolding, Δ_N^UASA (*44*), as

$$\Delta_N^U H^{hyd} = \Delta_N^U \mathrm{ASA}\,\Delta\bar{h} \qquad (6)$$

where $\Delta\bar{h}$ is the coefficient of proportionality and has units of J/(mol·Å^2). The Δ_N^UASA is defined as the difference in the solvent-accessible surface area of a group in the unfolded, ASA^U, and native, ASA^N, states:

$$\Delta_N^U \mathrm{ASA} = \mathrm{ASA}^U - \mathrm{ASA}^N \qquad (7)$$

For the 30/36 variants, the accessibility of residues Ile30 (0 Å^2) and Ile36 (25 Å^2) in the native state is very small, and the changes in Δ_N^UASA are entirely defined by the intrinsic ASA of the amino acid side chain in the unfolded state, i.e., $\Delta_N^U \mathrm{ASA} \approx \mathrm{ASA}^U$. The change in the enthalpy of unfolding upon substitution of residue A on residue B is therefore defined as

$$\Delta\Delta H^{exp}(\mathrm{A} \rightarrow \mathrm{B}) = \Delta H^{exp}(\mathrm{B}) - \Delta H^{exp}(\mathrm{A}) \qquad (8)$$

Each of the experimental enthalpies has a contribution from the internal interactions and from hydration, i.e.

$$\Delta H^{exp}(\mathrm{A}) = \Delta_N^U H^{int}(\mathrm{A}) + \Delta_N^U H^{hyd}(\mathrm{A}) \qquad (9)$$

and

$$\Delta H^{exp}(\mathrm{B}) = \Delta_N^U H^{int}(\mathrm{B}) + \Delta_N^U H^{hyd}(\mathrm{B}) \qquad (10)$$

The difference between these two equations will represent the difference in the enthalpy of internal interactions perturbed by A → B substitution and the enthalpy of hydration due to the difference in hydration of these two residues:

$$\Delta\Delta H^{exp}(\mathrm{A} \rightarrow \mathrm{B}) = \Delta\Delta_N^U H^{int}(\mathrm{A} \rightarrow \mathrm{B}) + \Delta\Delta_N^U H^{hyd}(\mathrm{A} \rightarrow \mathrm{B}) \qquad (11)$$

For the first term, $\Delta\Delta_N^U H^{int}(\mathrm{A} \rightarrow \mathrm{B})$, we can foresee that probably due to the significant changes in the shape and volume of the residues at the substitution sites there will be meaningful perturbations in the packing interactions at least in the vicinity of the mutation site. These changes will occur independently of whether the substitution made is to a smaller (Ile → Val), larger (Ile → Phe), or similar in size (Ile → Leu) residue. As already mentioned, there is currently not enough knowledge to predict, even on a qualitative level, changes in the internal interactions. For the second term, $\Delta\Delta_N^U H^{hyd}(\mathrm{A} \rightarrow \mathrm{B})$, the changes can be predicted. They will occur in proportion to the changes in ASA of the side chains or, if the side chain is fully buried in the native state, in proportion to the changes in the ASA of the side chain in the unfolded state, ASA^U, only, i.e.

$$\Delta\Delta_N^U H^{hyd}(\mathrm{A} \rightarrow \mathrm{B}) = [\Delta_N^U \mathrm{ASA}(\mathrm{B}) - \Delta_N^U \mathrm{ASA}(\mathrm{A})]\Delta\bar{h} = [\mathrm{ASA}^U(\mathrm{B}) - \mathrm{ASA}^U(\mathrm{A})]\Delta\bar{h} \qquad (12)$$

The ASA^U values for Val, Leu, Ile, and Phe are 117, 137, 140, and 175 Å^2, respectively (*44*). Simple estimates indicate that, for the Ile → Leu substitution, the contribution of hydration will be negligibly small

$$\Delta\Delta_N^U H^{hyd}(\mathrm{I} \rightarrow \mathrm{L}) = [\mathrm{ASA}^U(\mathrm{L}) - \mathrm{ASA}^U(\mathrm{I})]\Delta\bar{h} \approx 0 \qquad (13)$$

but will be sizable for all other substitutions. Thus in the case of the Ile → Leu substitution, the change in the internal interactions is not compensated by the changes in hydration. This simple analysis provides a *qualitative* explanation for the observed high instance of lower enthalpy of unfolding for variants containing Leu substitutions at either position 30 or 36. One needs to keep in mind that the substitutions cannot be isostructural and that they do perturb other interactions at least in the vicinity of the substitution site. We must also note that the amino acid substitutions might also perturb the structure of the unfolded state ensemble as

it was proposed in a number of studies (*47*−*55*). These perturbations in the structure are probably responsible for the overall unclear trends in the observed values of $\Delta\Delta^{U}_{N}H^{exp}$.

Effect of 30/36 Amino Acid Substitutions on the Stability. The second trend that is evident is that all substitutions lead to a *decrease* in the stability of the ubiquitin molecule. This can be interpreted as Ile's at positions 30 and 36 are the optimal residues for stability in the ubiquitin molecule. Ubiquitin is known to be one of the most conserved eukaryotic proteins. The difference in the 76-residue sequence between yeast and human ubiquitins is only three amino acid residues at solvent-exposed positions. Thus through evolution the sequence of ubiquitin was probably very carefully selected and preserved. The perturbations incorporated by the amino acid substitutions at positions 30 and 36 of the ubiquitin molecule must clearly affect the contribution of the hydrophobic interactions to the stability of this protein. It is known that the magnitude of hydrophobic interactions is proportional to the nonpolar water-accessible surface area (*43*, *44*, *56*−*59*). The trends we observe in the position 30/36 mutants clearly show that this is largely true. For example, the difference in the ΔG(50 °C) values between WT and 30V/36V is 7.8 kJ/mol. Knowing (*44*) the estimated values of the contribution of the hydrophobic effect to the protein stability expressed per unit of ASA, ∼185 J/(mol Å^2), estimates ∼42 Å^2 of the difference in the nonpolar surface area buried between WT and 30V/36V proteins. Theoretical estimates of the difference in the ASA between these two proteins, assuming that the two structures are identical except for positions 30 and 36, gives a value of 46 Å^2. This close correspondence of ASA change upon mutation can serve as an indirect support for the small structural differences between these two proteins.

The observed changes in the Gibbs energy change for 30/36 variants relative to the WT are in the range between 3 and 15 kJ/mol. These changes are much smaller than the changes in the enthalpy of unfolding, reaching to 40−50 kJ/mol. Interestingly, there is a weak correlation ($r^2 = 0.7$) between the changes in the enthalpy of unfolding and decrease in stability. Existence of such a correlation indicates that the decrease in stability is mostly enthalpic in nature. There are, however, changes in entropy which to some degree compensate for the unfavorable changes in the enthalpy of unfolding. Thus analysis of the nonpolar amino acid substitutions at the buried site in terms of not only the Gibbs energy but also the enthalpy and entropy can provide additional insight into the mechanisms of protein stabilization (*60*).

Interaction between the Residues at Positions 30 and 36. The estimates of different contributions to the stability of the ubiquitin variants assume that the contributions are additive. This appears to be valid for qualitative analysis. Quantitatively, however, there is always context dependence of the interactions. This can be evaluated from the so-called "double mutant cycle" (*61*) and has been used successfully before (e.g., ref *62*). The idea is to analyze the cyclic amino acid substitutions shown in Scheme 1. In this cycle the parallel pathways represent similar substitutions in the background of different protein variants. If the Gibbs energy for parallel pathways is the same, there is no interaction between sites A and B. Otherwise, there is a pairwise

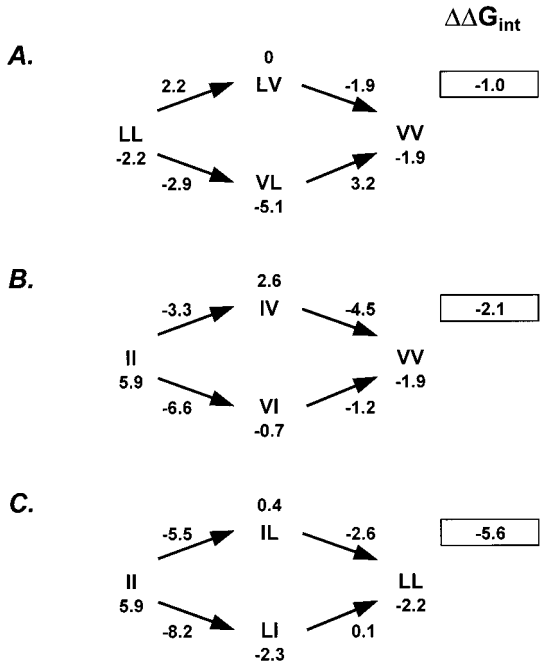

FIGURE 3: Evaluation of the pairwise interactions between positions 30 and 36 of ubiquitin at 50 °C and pH 3.0 and its dependence on the identity of amino acid residues using the double mutant cycle: (A) 30L/36L → 30V/36V; (B) 30I/36I → 30V/36V; (C) 30I/36I → 30L/36L. The pairwise interaction energy, $\Delta\Delta G_{int}$, is defined as a difference in the changes in the Gibbs energy upon substitution at positions 30 and 36, as shown by eq 14.

Scheme 1

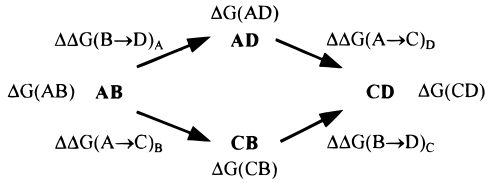

interaction between these two sites, and the energy of this interaction will be defined as the difference in the change in energy on the parallel pathways, i.e.

$$\Delta\Delta G_{int} = \Delta\Delta G(A \rightarrow C)_B - \Delta\Delta G(A \rightarrow C)_D = \Delta\Delta G(B \rightarrow D)_A - \Delta\Delta G(B \rightarrow D)_C \quad (14)$$

Such analysis performed for positions 30 and 36 shows (Figure 3) that indeed there are interactions between these sites with the pairwise energy ranging from relatively small, −1.0 and −2.4 kJ/mol, to quite significant, −5.6 kJ/mol. This indicates that the interactions at these two positions are strongly context dependent. The relative pairwise energy $\Delta\Delta G_{int}$ obtained using 30I/36I and 30V/36V or 30L/36L and 30V/36V pairs (Figure 3A,B) is relatively small, −2.1 and −1.0 kJ/mol, respectively. This can be considered as an indication that the presence of smaller side chains such as Val at positions 30 and 36 reduces the interactions between these two sites. Thus the pairwise energy is mainly reflecting the interactions between I30 and I36 or L30 and L36. In contrast, the $\Delta\Delta G_{int} = -5.6$ kJ/mol for the difference in the interactions between I30 and I36 versus L30 and L36 pair clearly indicates that the interactions between sites in 30L/36L are very unfavorable.

Having these double cycle mutants and making certain assumptions, we can also estimate the stability for the 30F/

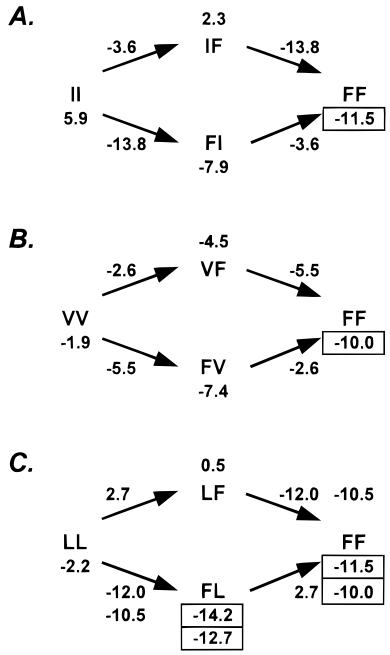

FIGURE 4: Estimation of the Gibbs energy of 30F/36F and 30F/36L variants of ubiquitin at 50 °C and pH 3.0 using the double mutant cycle: (A) 30I/36I → 30F/36F; (B) 30V/36V → 30F/36F; (C) 30L/36L → 30F/36F. The boxed values of the Gibbs energy are the estimated values. See text for details on the assumptions made for these estimates.

36L and 30F/36F variants. Due to the low solubility of these ubiquitin variants and their low intrinsic stability, experimental measurements of ΔG were not possible. Thus, the only way to estimate ΔG for the 30F/36L and 30F/36F variants is to use the known stabilities of other variants and assume the absence of pairwise interactions, i.e., $\Delta\Delta G_{int} = 0$. Even though this assumption is not valid in our case, it provides the upper limit estimate for the stability of these ubiquitin variants.

To estimate the stability of the 30F/36F variant of ubiquitin, we used two different double cycles (Figure 4A,B). We estimate that at 50 °C and pH 3.0 the stability for this variant of ubiquitin, ΔG(50 °C, pH 3.0), is between −11.5 and −10.0 kJ/mol. Relatively close (<20%) correspondence between two different double mutant cycles indirectly suggests that this estimate is tolerable. It must be emphasized that, due to the assumptions made, this estimate of ΔG will always be smaller than the actual decrease in stability. The stability of the 30F/36L variant was estimated as shown in Figure 4C, using the estimates for the 30F/36F variant. At 50 °C, ΔG for this variant is estimated to be between −14.2 and −12.7 kJ/mol, even lower than that for the 30F/36F variant. These estimates indicate that both the 30F/36F and 30F/36L variants of ubiquitin will be unfolded at pH 3.0 even at room temperature. This is exactly what is seen in the far-UV CD spectra for these proteins (Figure 2 and Table 2). There is clearly a difference between the spectra of the 30F/36F and 30F/36L variants and, for example, the wild-type protein, confirming their expected low stability. In particular, the decrease in $[\Theta]_{222}$ values and increase in R_2 parameter (see Table 2) can be considered as an indication that both of these variants of ubiquitin are largely unfolded under these (25 °C, pH 3.0) conditions.

Hydrophobic Interactions in Ubiquitin. Our results on the stability of the 30/36 hydrophobic ubiquitin variants favorably compare with the changes in stability as a result of similar substitutions in other proteins. The Ile → Val substitutions in ribonuclease T1 (*56*), ribonuclease A (*63*), staphylococcal nuclease (*64*), gene 5 protein (*65*), barnase (*66*), and T4 lysozyme (*67*, *68*) gave an average decrease in stability of -4.5 ± 1.8 kJ/mol at 25 °C (*69*). Similar results were obtained from the analysis of the Ile → Val substitution at five different positions of human lysozyme. Substitutions made in the background of wild-type protein lysozyme gave the values of $\Delta\Delta G = -3.2 \pm 1.5$ kJ/mol at 64 °C, whereas the changes in stability of $\Delta\Delta G = -3.6 \pm 1.6$ kJ/mol at 49 °C were obtained for the variants made in the background of three-disulfide human lysozyme (*27*). These values are in reasonable agreement with the changes in the stability of ubiquitin at 50 °C upon Ile → Val substitution in position 30 [$\Delta\Delta G$(30V/36I) = −6.6 kJ/mol], in position 36 [$\Delta\Delta G$(30I/36V) = −3.3. kJ/mol], or at both the 30 and 36 positions simultaneously [$\Delta\Delta G$(30V/36V) = −7.8 kJ/mol or −3.9 kJ/mol per one Ile → Val substitution].

The Ile → Phe substitutions have been previously generated only at two fully buried nonhelical positions in human lysozyme (*28*). The substitution at position 56 led to a significant decrease in stability at the reference temperature of 64 °C ($\Delta\Delta G = -17.1$ kJ/mol). In contrast, the substitution at position 59 led only to a moderate decrease in stability at 64 °C ($\Delta\Delta G = -3.4$ kJ/mol). A similar position-dependent difference in the change of stability upon Ile → Phe substitution is observed in our case as well. The I36F substitution in the molecule of ubiquitin (30I/36F) led to a decrease in stability of 3.6 kJ/mol, which compares well with the changes in stability upon I59F substitution in human lysozyme. The I30F substitution (30F/36I) leads to a much larger decrease in stability, on the order of −13.9 kJ/mol, which again is comparable to the decrease in stability upon similar amino acid substitution, I56F, in the molecule of human lysozyme. We believe that the difference in the loss of stability upon Ile → Phe substitutions at two buried positions can be explained by the local flexibility of the structure. Although in the native state side chains of amino acid residues at both the 30 and 36 positions are largely buried, they have different capabilities for accommodating larger and bulkier residues. Position 30 in the molecule of ubiquitin is in the last turn of an α-helix spanning residues 24−33. In Ile30, not only the side chain but also the backbone atoms are completely buried. Thus substitution of Ile30 with a much larger Phe residue will force the ubiquitin molecule to perturb its packing interaction to accommodate this much bulkier residue. Such motion will be quite costly energetically because this will most probably involve rearrangement away from the structurally rigid α-helix within the ubiquitin molecule. Isoleucine at position 36, on the other hand, is located in the loop connecting the α-helix with the following β-strand. In addition to the solvent exposure of the backbone of I36, the preceding residue in the sequence, Gly35, is also largely solvent exposed. Therefore, one can speculate that the substitution of Ile to Phe at position 36 will have a less dramatic effect on the stability because the strain imposed by the larger and bulkier Phe side chain can be relieved by the movement of the backbone atoms of the residues at positions 35 and 36. Thus, the decrease in stability upon I36F substitution in the 30I/36F variant will lead to only a moderate decrease in stability. Obviously, double Ile

→ Phe substitutions (i.e., 30F/36F) will lead to very dramatic decreases in stability which render the ubiquitin molecule extremely unstable. Even the most conservative estimates give the value of $\Delta\Delta G$(50 °C, pH 3.0) to be on the order of −19 kJ/mol for the 30F/36F variant relative to WT.

The Ile → Leu substitutions have been studied in two proteins, human lysozyme (*28*) and ribonuclease A (*63*). Analysis of the I56L and I59L substitutions in human lysozyme led to either no change [$\Delta\Delta G$(I59L) = 0 kJ/mol] or a small [$\Delta\Delta G$(I56L) = −0.4 kJ/mol] decrease in stability. In contrast, Ile → Leu substitutions in RNase A produced a 7.5 and 9.2 kJ/mol decrease in stability relative to the wild-type protein at 40 °C (*63*). Similarly, the 30L/36I ubiquitin variant is 7.7 kJ/mol less stable than the WT, whereas the 30I/36L variant is 5.5 kJ/mol less stable. Such a decrease in stability should not be surprising for the reasons discussed above; i.e., both residues have similar energetics of hydration but will differ in the packing interactions in the native state. There is more evidence that Ile → Leu substitution is not isoenergetic and should lead to a change in stability despite the similarities of these aliphatic side chains in their interactions with the solvent water, i.e., thermodynamics of hydration (*44*). First, the difference in the configurational entropies of Ile and Leu is quit significant (*70*, *71*). Second, recent studies on the helical peptide by Luo and Baldwin (*37*) show that Ile and Leu are different not only in terms of their helix-forming propensities but also in the enthalpy of helix formation.

Concluding Remarks. Detailed thermodynamic analyses of 16 variants that differ in hydrophobic contact located at the C-terminus of an α-helix of the ubiquitin molecule have been performed. It has been shown that the wild-type interactions that contain isoleucine residues are the most stabilizing. Introduction of leucine, valine, or phenylalanine leads to a decrease of stability, in some cases so dramatic that it renders an unfolded protein. In the case of isoleucine to leucine substitutions the decrease in stability is also accompanied by a significant (up to 25%) decrease in the enthalpy of unfolding. This decrease in the enthalpy is proposed to be due to the perturbed packing in the structure of ubiquitin variants. The decrease in the stability upon substitutions in the 30/36 hydrophobic contact in ubiquitin does not, however, seem to have a significant effect on the secondary structure content as measured by CD spectroscopy. This suggests that the hydrophobic contact at the C-terminus of the α-helix might be important for the stability of the structure.

REFERENCES

1. Baldwin, R. L., and Rose, G. D. (1999) *Trends Biochem. Sci. 24*, 26−33.
2. Baldwin, R. L., and Rose, G. D. (1999) *Trends Biochem. Sci. 24*, 77−83.
3. Aurora, R., and Rose, G. D. (1998) *Protein Sci. 7*, 21−38.
4. Pauling, L., and Corey, R. B. (1951) *Proc. Natl. Acad. Sci. U.S.A. 37*, 241−250.
5. Presta, L. G., and Rose, G. D. (1988) *Science 240*, 1632−1641.
6. Richardson, J. S., and Richardson, D. C. (1988) *Science 240*, 1648−1652.
7. Gong, Y., Zhou, H. X., Guo, M., and Kallenbach, N. R. (1995) *Protein Sci. 4*, 1446−1456.
8. Sukumar, M., and Gierasch, L. M. (1997) *Folding Des. 2*, 211−222.
9. Viguera, A. R., and Serrano, L. (1995) *J. Mol. Biol. 251*, 150−160.
10. Khorasanizadeh, S., Peters, I. D., Butt, T. R., and Roder, H. (1993) *Biochemistry 32*, 7054−7063.
11. Makhatadze, G. I., Lopez, M. M., Richardson, J. M., III, and Thomas, S. T. (1998) *Protein Sci. 7*, 689−697.
12. Di Stefano, D. L., and Wand, A. J. (1987) *Biochemistry 26*, 7272−7281.
13. Vijay-Kumar, S., Bugg, C. E., Wilkinson, K. D., Vierstra, R. D., Hatfield, P. M., and Cook, W. J. (1987) *J. Biol. Chem. 262*, 6396−6399.
14. Cormack, B. (1992) in *Short protocols in molecular biology* (Ausubel, F. M., Brent, R., Moore, D. D., Seidman, J. G., Smith, J. A., and Struhl, K., Eds.) pp 818−825, John Wiley & Sons, New York.
15. Loladze, V. V., Ibarra-Molero, B., Sanchez-Ruiz, J. M., and Makhatadze, G. I. (1999) *Biochemistry 38*, 16419−16423.
16. Gribenko, A. V., and Makhatadze, G. I. (1998) *J. Mol. Biol. 283*, 679−694.
17. Makhatadze, G. I. (1998) *Measuring protein thermostability by differential scanning calorimetry*, Vol. 2, John Wiley & Sons, New York.
18. Makhatadze, G. I., Medvedkin, V. N., and Privalov, P. L. (1990) *Biopolymers 30*, 1001−1010.
19. Winder, A. F., and Gent, W. L. (1971) *Biopolymers 10*, 1243−1251.
20. Ibarra-Molero, B., Makhatadze, G. I., and Sanchez-Ruiz, J. M. (1999) *Biochim. Biophys. Acta 1429*, 384−390.
21. Makhatadze, G. I. (1999) *J. Phys. Chem. 103*, 4781−4785.
22. Makhatadze, G. I. (1998) *Biophys. Chem. 71*, 133−156.
23. Shortle, D., Meeker, A. K., and Freire, E. (1988) *Biochemistry 27*, 4761−4768.
24. Tanaka, A., Flanagan, J., and Sturtevant, J. M. (1993) *Protein Sci. 2*, 567−576.
25. Carra, J. H., Anderson, E. A., and Privalov, P. L. (1994) *Biochemistry 33*, 10842−10850.
26. Carra, J. H., and Privalov, P. L. (1995) *Biochemistry 34*, 2034−2041.
27. Takano, K., Ogasahara, K., Kaneda, H., Yamagata, Y., Fujii, S., Kanaya, E., Kikuchi, M., Oobatake, M., and Yutani, K. (1995) *J. Mol. Biol. 254*, 62−76.
28. Funahashi, J., Takano, K., Yamagata, Y., and Yutani, K. (1999) *Protein Eng. 12*, 841−850.
29. Takano, K., Yamagata, Y., Fujii, S., and Yutani, K. (1997) *Biochemistry 36*, 688−698.
30. Kuroki, R., Inaka, K., Taniyama, Y., Kidokoro, S., Matsushima, M., Kikuchi, M., and Yutani, K. (1992) *Biochemistry 31*, 8323−8328.
31. Woody, R. W. (1985) in *The peptides* (Gross, E., and Meienhofer, J., Eds.) John Wiley & Sons, New York.
32. Chakrabartty, A., Doig, A. J., and Baldwin, R. L. (1993) *Proc. Natl. Acad. Sci. U.S.A. 90*, 11332−11336.
33. Munoz, V., and Serrano, L. (1995) *Curr. Opin. Biotechnol. 6*, 382−386.
34. Myers, J. K., Pace, C. N., and Scholtz, J. M. (1997) *Biochemistry 36*, 10923−10929.
35. Pace, C. N., and Scholtz, J. M. (1998) *Biophys. J. 75*, 422−427.
36. Scholtz, J. M., and Baldwin, R. L. (1992) *Annu. Rev. Biophys. Biomol. Struct. 21*, 95−118.
37. Luo, P., and Baldwin, R. L. (1999) *Proc. Natl. Acad. Sci. U.S.A. 96*, 4930−4935.
38. Richardson, J. M., McMahon, K. W., MacDonald, C. C., and Makhatadze, G. I. (1999) *Biochemistry 38*, 12869−12875.
39. Stellwagen, E., Park, S. H., Shalongo, W., and Jain, A. (1992) *Biopolymers 32*, 1193−1200.
40. Lyu, P. C., Liff, M. I., Marky, L. A., and Kallenbach, N. R. (1990) *Science 250*, 669−673.
41. Pain, R. (1998) in *Current Protocols in Protein Chemistry*, pp 721−723, John Wiley & Sons, New York.
42. Bruch, M. D., Dhingra, M. M., and Gierasch, L. M. (1991) *Proteins: Struct., Funct., Genet. 10*, 130−139.
43. Lazaridis, T., Archontis, G., and Karplus, M. (1995) *Adv. Protein Chem. 47*, 231−306.

44. Makhatadze, G. I., and Privalov, P. L. (1995) *Adv. Protein Chem. 47*, 307−425.
45. Richards, F. M., and Lim, W. A. (1993) *Q. Rev. Biophys. 26*, 423−498.
46. Rose, G. D., and Wolfenden, R. (1993) *Annu. Rev. Biophys. Biomol. Struct. 22*, 381−415.
47. Dill, K. A., and Shortle, D. (1991) *Annu. Rev. Biochem. 60*, 795−825.
48. Stigter, D., Alonso, D. O., and Dill, K. A. (1991) *Proc. Natl. Acad. Sci. U.S.A. 88*, 4176−4180.
49. Barbar, E., Barany, G., and Woodward, C. (1996) *Folding Des. 1*, 65−76.
50. Shortle, D., Chan, H. S., and Dill, K. A. (1992) *Protein Sci. 1*, 201−215.
51. Lattman, E. E., Fiebig, K. M., and Dill, K. A. (1994) *Biochemistry 33*, 6158−6166.
52. Saab-Rincon, G., Gualfetti, P. J., and Matthews, C. R. (1996) *Biochemistry 35*, 1988−1994.
53. Matthews, B. W. (1996) *FASEB J. 10*, 35−41.
54. Giletto, A., and Pace, C. N. (1999) *Biochemistry 38*, 13379−13384.
55. Wong, K. B., Clarke, J., Bond, C. J., Neira, J. L., Freund, S. M., Fersht, A. R., and Daggett, V. (2000) *J. Mol. Biol. 296*, 1257−1282.
56. Pace, C. N. (1992) *J. Mol. Biol. 226*, 29−35.
57. Yang, A. S., Sharp, K. A., and Honig, B. (1992) *J. Mol. Biol. 227*, 889−900.
58. Lee, B. (1993) *Protein Sci. 2*, 733−738.
59. Hummer, G., Garde, S., Garcia, A. E., Paulaitis, M. E., and Pratt, L. R. (1998) *Proc. Natl. Acad. Sci. U.S.A. 95*, 1552−1555.
60. Makhatadze, G. I., Clore, G. M., and Gronenborn, A. M. (1995) *Nat. Struct. Biol. 2*, 852−855.
61. Horovitz, A., and Fersht, A. R. (1992) *J. Mol. Biol. 224*, 733−740.
62. Hillier, B. J., Rodriguez, H. M., and Gregoret, L. M. (1998) *Folding Des. 3*, 87−93.
63. Torrent, J., Connelly, J. P., Coll, M. G., Ribo, M., Lange, R., and Vilanova, M. (1999) *Biochemistry 38*, 15952−15961.
64. Shortle, D., Stites, W. E., and Meeker, A. K. (1990) *Biochemistry 29*, 8033−8041.
65. Sandberg, W. S., and Terwilliger, T. C. (1991) *Proc. Natl. Acad. Sci. U.S.A. 88*, 1706−1710.
66. Kellis, J. T., Jr., Nyberg, K., and Fersht, A. R. (1989) *Biochemistry 28*, 4914−4922.
67. Eriksson, A. E., Baase, W. A., Zhang, X. J., Heinz, D. W., Blaber, M., Baldwin, E. P., and Matthews, B. W. (1992) *Science 255*, 178−183.
68. Matsumura, M., Becktel, W. J., and Matthews, B. W. (1988) *Nature 334*, 406−410.
69. Pace, C. N. (1995) *Methods Enzymol. 259*, 538−554.
70. Creamer, T. P., and Rose, G. D. (1992) *Proc. Natl. Acad. Sci. U.S.A. 89*, 5937−5941.
71. Creamer, T. P., and Rose, G. D. (1994) *Proteins 19*, 85−97.

BI0000418